Polímeros: Ciência e Tecnologia
E-ISSN: 1678-5169
abpol@abpol.org.br
Associação Brasileira de Polímeros
Brasil

de Farias, Marcelo Alexandre; do Carmo Gonçalves, Maria
Synthesis and applications of polystyrene-block-poly(N-vinyl-2-pyrrolidone) copolymers
Polímeros: Ciência e Tecnologia, vol. 26, núm. 1, enero-febrero, 2016, pp. 1-10
Associação Brasileira de Polímeros
São Carlos, Brasil

http://dx.doi.org/10.1590/0104-1428.2066

Synthesis and applications of polystyrene-*block*-poly(N-vinyl-2-pyrrolidone) copolymers

Marcelo Alexandre de Farias[1]* and Maria do Carmo Gonçalves[1]

[1]Institute of Chemistry, Universidade Estadual de Campinas – UNICAMP, São Paulo, SP, Brazil

**marcelo.adf@gmail.com*

Abstract

This work describes the synthesis and applications of amphiphilic polystyrene-*block*-poly(N-vinyl-2-pyrrolidone) (PS-*b*-PVP) copolymers as a silver and silica nanoparticle surface modification agent. The synthesis of PS-*b*-PVP was carried out using controlled/living radical polymerization techniques. The synthesis of the block copolymers was confirmed by gel permeation chromatography and hydrogen nuclear magnetic resonance, presenting a polydispersity index of around 1.4 and number average molecular weight ranging between 10,000-14,000 g mol^{-1}. The PS-*b*-PVP copolymers were applied as a silver nanoparticle (AgNP) stabilizing agent. These nanoparticles were produced by a single step and presented an 11 ± 1 nm diameter. Furthermore, the PS-*b*-PVP copolymers were also applied as a silica nanoparticle (SiO_2NP) surface modification agent. The SiO_2NP were synthesized by the Stöber method presenting a 72 ± 9 nm diameter. The SiO_2NP surface modification by adsorption of PS-*b*-PVP caused the formation of a 5 ± 1 nm thick polymeric layer, providing the SiO_2NP with a hydrophobic surface character. The structural and chemical characteristics shown by PS-*b*-PVP copolymers highlights their versatility for several applications, such as: water-in-oil emulsifier, stabilizing or coupling agents between inorganic particles and polymeric matrices.

Keywords: *amphiphilic block copolymers, controlled radical polymerization, silica nanoparticles, silver nanoparticles, surface modification agent.*

1. Introduction

Currently, using controlled/living radical polymerization (CRP) techniques, efforts in new polymer structures are focused on producing amphiphilic block copolymers[1-3]. These macromolecules are made up of two chemically different homopolymer blocks (A and B) combined as AB or ABA: one being hydrophilic and the other being hydrophobic. Polystyrene is a classic example of a hydrophobic glassy polymer frequently synthesized via CRP techniques[4–7]. On the other hand, an example of hydrophilic polymer is poly(N-vinyl-2-pyrrolidone) (PVP) which has been synthesized via CRP in the last few years[8-10]. PVP is an important building block and has attracted significant attention from the biomedical field because it is biocompatible and non-toxic, being an excellent candidate to replace PEO in certain biomaterial applications[8]. Furthermore, PVP is also known for its ability to easily form complexes with metals[11].

Amphiphilic block copolymers, when dissolved in a selective solvent, tend to self-assemble producing core-shell micelles. These micelles are capable of encapsulating metallic particles obtained from their metal salts[12]. In this case, the core block is able to entrap particles by complexation or association, and the shell block provides a hydrophobic or hydrophilic character for the colloidal nanoparticle. Furthermore, several experimental and theoretical studies have been reported in relation to the surface modification by block copolymers in order to promote specific characteristics[12–15]. Zhang et al.[16] used poly(ethylene oxide)-*block*-poly(methyl methacrylate) (PEO-*b*-PMMA) copolymer as a template for the synthesis of silver nanowires in an aqueous solution. In this system, the PMMA block reduces silver ions and PEO block promotes the nanoparticle dispersion in water. Li et al.[17] modified the surface of Fe_3O_4 magnetic nanoparticles with amphiphilic poly(*tert*-butyl methacrylate)-*block*-poly(glycidyl methacrylate) (P*t*BMA-*b*-PGMA) in order to improve the microwave-assisted extraction of polycyclic aromatic hydrocarbons (PAH) in environmental water. The P*t*BMA block provides a highly hydrophobic property for the Fe_3O_4 magnetic nanoparticles responsible for adsorbing PAH. On the other hand, the PGMA block is responsible for the immobilization of the block copolymer on the magnetic nanoparticles. The authors observed that the extraction of PAH is improved when Fe_3O_4 magnetic nanoparticles are encapsulated by P*t*BMA-*b*-PGMA.

Amphiphilic copolymers of polystyrene-*block*-poly(N-vinyl-2-pyrrolidone) (PS-*b*-PVP) have been reported employing the following radical polymerizations: pseudo-living[18], atom transfer radical polymerization (ATRP)[9,19], ATRP followed by reversible addition−fragmentation chain-transfer polymerization (RAFT)[20], RAFT[21], RAFT followed by ATRP[22], nitroxide-mediated polymerization (NMP)[23,24], organostibine-mediated[25] and organogermanium-mediated polymerizations[26]. Although PS-*b*-PVP copolymers have been synthesized by several methods, some did not provide suitable PS-*b*-PVP amphiphilic copolymers due to the presence of homopolymers as impurities and high Đ values (i.e. > 2.0)[18,26] and others involve complex experimental steps in order to produce intermediate species (e.g. synthesis of mediators and chain transfer agents)[21,25]. Furthermore, the PS-*b*-PVP copolymer is not commercially available and has potential applications in polymer science (e.g. stabilization, dispersibility, emulsifier, coupling agents), which are not sufficiently exploited.

In this work, we describe the synthesis of amphiphilic PS-*b*-PVP copolymers by RAFT and their application as a silver and silica nanoparticle stabilizing or a surface modification agent, respectively. Although RAFT technique has the advantage of being applicable to a much wider variety of monomers than the ATRP technique, usually the synthesis of RAFT end-functionalized initiators (chain transfer agents) is not so simple[21]. For this reason, styrene was initially synthesized in bulk by ATRP leading to polystyrene with bromine chain end functionality. Then, a suitable macro chain transfer agent (macro-CTA) was formed by performing a simple method[20,27] to convert the polystyrene ATRP product into the RAFT agent. N-vinyl-2-pyrrolidone (VP) was subsequently used as a chain extensor of this RAFT agent to synthesize well-defined amphiphilic PS-*b*-PVP copolymers. Applying this methodology, the use of toxic solvents or complex experimental steps was avoided.

The block copolymers produced were structurally characterized by hydrogen nuclear magnetic resonance (^{1}H NMR) and gel permeation chromatography (GPC). Thermal properties were evaluated by differential scanning calorimetry (DSC). Furthermore, the PS-*b*-PVP copolymers were applied not only to stabilize *in-situ* prepared silver nanoparticles (AgNP) but were also used to modify the silica nanoparticle (SiO_2NP) surface in order to show specific applications for these copolymers.

2. Materials and Methods

2.1 Materials

Styrene (>99%), N-vinyl-2-pyrrolidone (VP, >99%), copper(I) bromide (CuBr, 98%), 5,5′-dimethyl-2,2′-dipyridyl (98%), potassium ethyl xanthogenate (96%), (1-bromoethyl) benzene (97%), dimethylacetamide (DMAc), tetraethyl orthosilicate (TEOS, 98%) and 2,2′-azobis(2-methylpropionitrile) solution (AIBN, 0.2 mol L^{-1} in toluene) were purchased from Aldrich. Acetone, ethanol, methanol, ammonium hydroxide solution (27%), silver nitrate ($AgNO_3$), sodium hydroxide (NaOH), dimethylacetamide (DMAc) and tetrahydrofuran (THF) were purchased from Vetec-Sigma (Brazil).

2.2 Removal of inhibitors present in the monomers

Equal volumes of styrene and aqueous NaOH solution (10% w/v) were vigorously stirred in a 500 mL separation funnel. Then, phase separation was observed and the bottom phase was discarded. The upper phase was washed three times with distilled water, always discarding the bottom phase. After, the styrene fraction was distilled at 40 ± 2 °C and the pure styrene was collected in a flask immersed in liquid nitrogen. The VP monomer was distilled under vacuum using a Vigreux column. The initial distillation temperature was 90 °C being gradually increase up to 100 °C.

2.3 Preparation of PS-Br homopolymer via ATRP

The [monomer]:[initiator]:[CuBr]:[ligand] ratios used in this section, according to Hayes and Rannard[28], were 96:1:1:2.5. Additionally, an identical synthesis was carried out in the same ratio, except for the monomer to initiator ratio, which was 192:1.

Styrene (10.0 mL, 87.5 mmol) and (1-bromoethyl)benzene (0.124 mL, 0.909 mmol) were added to a Schlenk flask under continuous argon flux (positive pressure). The mixture was degassed by four freeze-pump-thaw cycles. After each thaw, the Schlenk was opened under argon flux (5 seconds), to remove the released gases from the solution and again closed under argon atmosphere. Then, CuBr (0.130 g, 0.909 mmol) and 5,5′-dimethyl-2,2′-dipyridyl (0.418 g, 2.27 mmol) were introduced into the frozen mixture under argon flux. The mixture was degassed by further two freeze-pump-thaw cycles. The Schlenk flask was then immersed in a pre-heated oil bath at 110 °C. After 18 h, THF (20.0 mL) was added to solubilize the solid product. The resulting mixture was permeated through a column filled with alumina (0.15 m length), using THF as an eluent in order to remove the metal complex catalyst from the polymeric solution. The polymeric solution was precipitated in methanol followed by drying under vacuum at 40 °C until reaching constant mass, thus obtaining a white solid product (PS-Br).

2.4 Preparation of amphiphilic PS-b-PVP copolymer via RAFT

Macro-CTA was prepared by ionic substitution reaction, similar to a previously reported procedure[20,27]. In a two neck round bottom flask, potassium ethyl xanthogenate (0.267 g, 1.66 mmol) was dissolved in acetone (6.00 mL). Then, PS-Br (1.00 g) was dissolved in THF (5.00 mL) and added dropwise in the two neck round bottom flask under argon flux. This solvent mixture can be considered a good solvent for the components. The reaction was conducted at room temperature (25 ± 5 °C) overnight. To obtain the solid macro-CTA (PS-xanthogenate), the solution was precipitated in methanol followed by drying under vacuum at 40 °C until constant mass was obtained.

The synthesis of the amphiphilic PS-*b*-PVP copolymer followed the traditional bulk RAFT polymerization. Macro-CTA (1.0 g) and VP monomer (15.0 mL) were added in a Schlenk flask under continuous argon flow. The mixture was degassed by four freeze-pump-thaw cycles. Then, AIBN (0.198 mL, 0.0289 mmol) was introduced into the Schlenk flask under continuous argon flux. The mixture was degassed by further two freeze-pump-thaw cycles. The Schlenk flask was then immersed in a pre-heated oil bath at 70 °C for 48 h. Then, the viscous solution was precipitated in water, followed by centrifugation (13,500 rpm for 10 min) and drying under vacuum at 40 °C until constant mass was reached. Thus, the white solid product was purified by solubilization in THF, precipitation in distilled water, centrifugation and drying under the same conditions cited before.

2.5 Synthesis of silver nanoparticles using a PS-b-PVP copolymer

A PS-*b*-PVP copolymer was used as a stabilizing agent in silver nanoparticle (AgNP) synthesis. In a typical experiment, 50 mg of PS-*b*-PVP copolymer were added to 10 mL of dimethylacetamide (DMAc) under stirring. Afterwards, 0.1 mL of aqueous NaOH (0.1 mol L^{-1}) and 0.1 mL of aqueous $AgNO_3$ (0.1 mol L^{-1}) solutions were added drop-wise in 5 minute intervals. The colloidal suspension remained under magnetic stirring for a further 20 minutes.

2.6 Synthesis of silica nanoparticles and PS-b-PVP copolymer adsorption

Silica nanoparticles (SiO_2NP) were prepared by the classical Stöber method[29]. Briefly, 2 mL of TEOS were added to 25 mL of ethanol within screw-cap vials, in the presence of 10.5 mmol of ammonium hydroxide solution. The alcoholic solution was kept under ultrasonic bath (25 kHz-200W) for 120 min at 30 °C[30]. The solid content was determined gravimetrically by drying the dispersion at 80 °C until a constant weight was obtained. The modification of SiO_2NP was carried out as follows: a SiO_2NP dispersion (1) was prepared by the addition of SiO_2NP (50 mg) to a flask containing DMAc (10 mL) in an ultrasonic bath; a PS-*b*-PVP solution (2) was prepared by the dissolution of PS-*b*-PVP copolymers (50 mg) in DMAc (5 mL). Then, the solution (2) was slowly added to the dispersion (SiO_2NP/DMAc) (1) under ultrasonic bath. After 48 h, the resulting dispersion was centrifuged at 14,000 rpm for 20 minutes. The supernatant containing excess of PS-*b*-PVP copolymer was removed and the precipitated solid (SiO_2NP coated by PS-*b*-PVP copolymer) was lyophilized.

2.7 Characterization

^{1}H NMR spectra of the polymers were obtained in deuterated chloroform solutions ($CDCl_3$) using a Bruker Avance III - 600MHz spectrometer operating at 600 MHz. Gel permeation chromatography (GPC) measurements were performed using a Viscotek GPCmax VE 2001, equipped with Viscotek VE 3580 RI Detector and three Shodex KF-8060M columns working at 40 °C. Degassed THF was used as an eluent (1 mL min^{-1}) and as a solvent to prepare 8.0 mg mL^{-1} sample solutions. Homopolymer and block copolymer molecular weights were determined using polystyrene standards. DSC analyses were performed with TA instruments DSC-Q100 in nitrogen atmosphere. Samples of ca. 5 mg were heated from 25 to 200 °C, cooled from 200 to -10 °C and heated from -10 to 200 °C at a heating rates of 10 °C min^{-1}. TEM images were obtained using a Carl Zeiss LIBRA 120 PLUS operating at 120 kV and equipped with in-column OMEGA energy filter (EF-TEM). Samples were prepared by dropping 20 µL of a DMAc dispersion containing AgNP or SiO_2NP in copper grid coated with thin amorphous carbon. Electron spectroscopic imaging (ESI-TEM) was carried out for carbon mapping. The absorption spectra of colloidal Ag were obtained with an Agilent Cary 50 Probe ultraviolet–visible spectrophotometer using 0.5 mL of colloidal suspension diluted to 2.5 mL of DMAc.

3. Results and Discussion

3.1 Amphiphilic PS-b-PVP copolymers

The synthesis of PS-Br homopolymers via ATRP is a well-established methodology in literature. According to ^{1}H NMR measurements (not shown here) the chain end functionality of the homopolymers synthesized was confirmed by the signals at 4.60-4.35 ppm attributed to the hydrogen located in the α position of the bromine chain end. Based on the signal intensity ratios between the 7.37-6.21 ppm range and those in the 4.60-4.35 ppm range, the calculated molecular weights by ^{1}H NMR (M_{NMR}), considering the ratio monomer:bromine chain end, were ca. 9,500 g mol^{-1} and 12,700 g mol^{-1}, corresponding respectively to the PS_{91}-Br and PS_{122}-Br copolymers. Further M_n and Đ values obtained by GPC for the homopolymers and block copolymers synthesized, are shown in Table 1.

The M_{NMR} value represents the ratio of monomer units per bromine chain end. Depending on the application or the properties of interest, the use of the ratio between each block in the final amphiphilic block copolymer (e.g. 2:1 hydrophobic:hydrophilic block ratio) instead of the characteristic size of this block copolymer is more appropriate. For this reason, in the present work, we adopt the M_{NMR} value because the resulting ratios of each block better represents the structural characteristics of the amphiphilic PS-*b*-PVP copolymer, since applications as coupling agent, surfactants, emulsifier or self-assembly micelles in selective solvent solutions are considered.

The bromide PS chain end group was converted to xanthogenate by an ionic substitution reaction, producing a suitable macro chain transfer agent (macro-CTA) for the PS-*b*-PVP polymerization. Hussain et al.[20] produced amphiphilic PS-*b*-PVP copolymer starting from PS obtained by ATRP followed by RAFT of PVP. The authors used acetone as the solvent for conversion of the ATRP product (PS-Br) into RAFT macro-CTA, however acetone is not a solvent for this homopolymer[31]. Thus, in the present work, we used THF as it is a good solvent for polystyrene conversion into macro-CTA, avoiding phase separation and consequently low conversion yields due the higher molar masses of PS presented here. Similar conversion of the ATRP initiators into their corresponding RAFT macro-CTA was demonstrated by Wager et al.[27] applying modified ATRP conditions for polymer chain activation in presence of bis(thiobenzoyl) disulphide. Thus, the bromine chain end of poly(methylmethacrylate), poly(N,N-dimethylaminoethyl methacrylate) and poly(ethylene glycol) produced by ATRP were converted with high yields into to the desired RAFT end-functionality.

Table 1. Molecular parameters obtained for the homopolymers and block copolymers.

Polymer	M_{NMR} (g mol^{-1})	M_n [a] (g mol^{-1})	Đ [a]	Mass Yield (%) [b]	PS mass fraction [c]
PS_{91}-Br	9,500	5,800	1.5	73	-
PS_{122}-Br	12,700	9,600	1.2	68	-
PS_{91}-*b*-PVP_{73}	17,600	10,500	1.5	65	0.55
PS_{122}-*b*-PVP_{70}	20,500	13,900	1.4	69	0.64

[a]Determined by GPC with THF as the eluente with respect to polystyrene standards. [b]Calculated after purification. [c]Determined by ^{1}H NMR.

In this work, a xanthate containing an alkali metal (potassium) as R group was used to react with the PS homopolymer containing a halogen (bromine) as the chain end group, synthesized by ATRP. An ionic substitution reaction is easily carried out with these groups using adequate solvent for each species or a combination of solvents as used here. Based on this, we believe that the methodology used herewith can be applied to a vast range of other combinations of xanthates containing alkali metals as the R group and homopolymers synthesized by ATRP, thus leading to a great variety of functional macro-CTA appropriate to the RAFT technique. The key role of the RAFT technique is the appropriate choice and synthesis of the so-called CTA or macro-CTA[7,8], thus in this step, the PS xanthogenate chain end was used for the subsequent chain extension with the VP monomer in absence of solvent.

The amphiphilic PS-*b*-PVP copolymer was initially synthesized via ATRP followed by RAFT for two reasons: (i) styrene is easily synthesized by ATRP technique, and in this case, the polymerization was conducted in bulk (solvent free); (ii) using only RAFT to synthesize PS homopolymer and subsequent PS-*b*-PVP copolymer would surely cause solubility problems due to the copolymer amphiphilic character. Furthermore, one could also point out the use of non-environmentally friendly solvents.

Figure 1 shows the ^{1}H NMR spectra of the synthesized amphiphilic PS-*b*-PVP copolymers. The PS hydrogen signals were assigned with "b", "c", "d", "e" and "f", xanthate hydrogen signals were assigned with "g" and "h", and the PVP hydrogen signals were assigned with "i", "j", "k", "l", "o" and "p". These assignments are also in agreement with literature[20,21,23,32]. Based on the signal intensity ratios between the 7.37–6.21 ppm range and those attributed only to PVP block (3.30 ppm and 3.90-3.55 ppm range), both copolymers were made up of around 70 VP monomeric units. The calculated M_{NMR} of the block copolymers were ca. 17,600 g mol^{-1} and 20,500 g mol^{-1} corresponding to PS_{91}-*b*-PVP_{73} and PS_{122}-*b*-PVP_{70} copolymers, respectively. Regarding the macro-CTA with the lowest molecular weight (PS_{91}-xanthogenate), the PS_{91}-*b*-PVP_{73} copolymer molecular weight almost doubled compared to the respective homopolymer, corresponding to 0.55 PS mass fraction. Furthermore, no difference in Đ was observed, which remained the same for the homo and block copolymers. On the other hand, in relation to the macro-CTA with the highest molecular weight (PS_{122}-xanthogenate), a slight increase in Đ was observed from the 1.2 to 1.4 and the corresponding block copolymer (PS_{122}-*b*-PVP_{70}) exhibited a 0.64 PS mass fraction.

GPC curves of homopolymers and the respective block copolymer are shown in Figure 2. The GPC results of PS-Br and PS-*b*-PVP copolymers displayed unimodal curves. The significant shift in these curves indicates a successful increase in the block copolymer molecular weights in relation to the original homopolymers. Other copolymers reported in literature, where the VP monomer was polymerized via RAFT from the PS macro-CTA, show low yields[33] or similar Đ values[21]. Bilalis et al.[23] synthesized VP block copolymers using styrene and 2-vinylpyridine via NMP and RAFT techniques, respectively. Applying the NMP technique, yields ranging from 20 to 70% were obtained, however a 2.2 Đ value was observed for the block copolymer with the highest yield. RAFT technique also provided similar results in relation to NMP, achieving yields ranging from 10 to 65% and 2.1 Đ value. The lowest Đ value (Đ = 1.4) was reached when PS was used as the first polymerized block followed by diblock synthesis with VP monomer addition. This value is in agreement with the results presented in Table 1.

GPC measurements indicated that PS_{91}-Br and PS_{122}-Br presented 1.5 and 1.2 Đ values, respectively (Table 1). One of the literature criteria used to define a controlled polymerization is based on the Đ values, where $M_w/M_n \leq 1.5$ is considered a narrow molecular weight distribution[4,34-36]. Normally, very narrow Đ values ($M_w/M_n \leq 1.2$) are obtained at low monomer conversion rates and/or by using solvent in the polymerization[25,37,38]. In the present work, we conducted the PS polymerization in bulk resulting Đ values slightly above very narrow Đ values ($M_w/M_n \leq 1.2$) but still in the range of CRP Đ values ($M_w/M_n \leq 1.5$).Thus, this work is in agreement with literature reported Đ values[4,6,20-22,25,35].

DSC heating curves of the PS-*b*-PVP copolymers is shown in Figure 3. Only the second heating scan curves

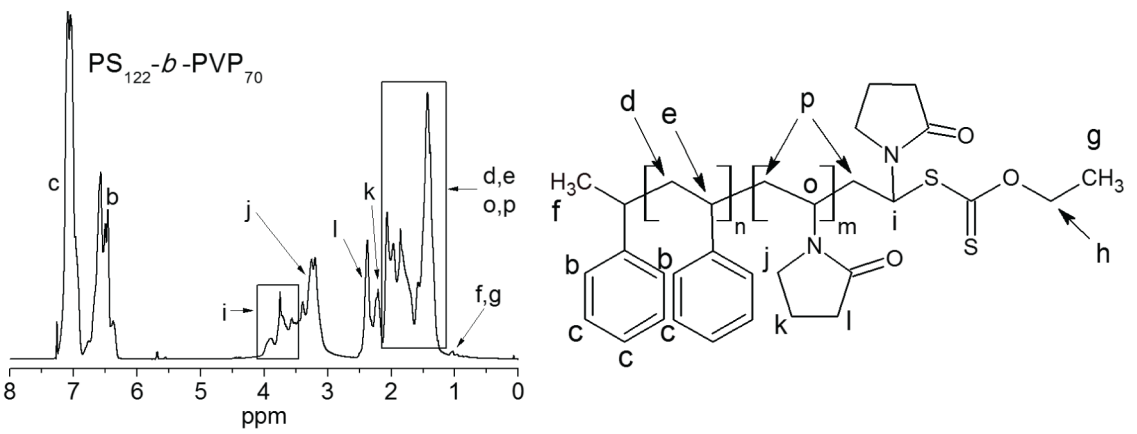

Figure 1. ^{1}H NMR spectra of amphiphilic PS_{122}-*b*-PVP_{70} copolymer and the corresponding peak assignments.

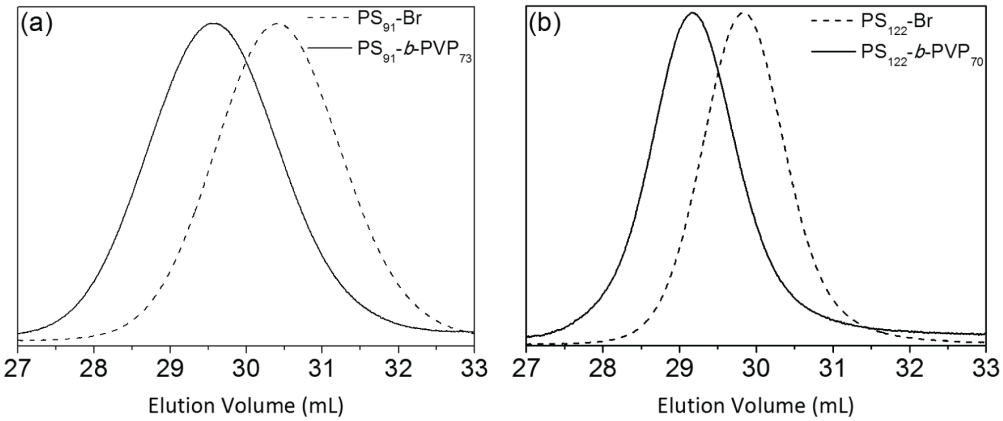

Figure 2. Comparison of GPC curves of (a) the lower and (b) the higher homopolymers with the corresponding block copolymers.

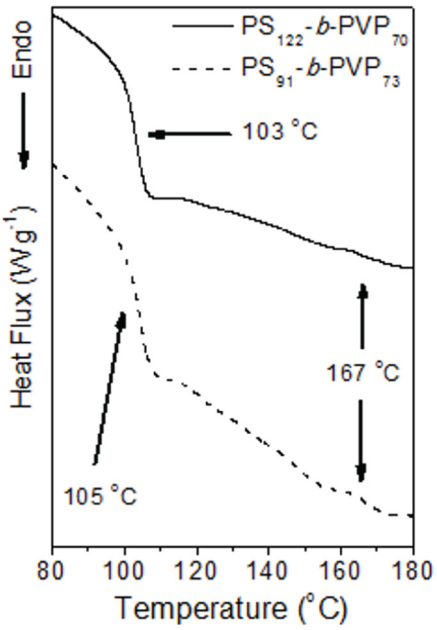

Figure 3. DSC curves of the amphiphilic PS-b-PVP copolymers. The arrows show the Tg values of PS and PVP blocks.

are shown due to fact that they establish a defined sample history. Initially, the PS homopolymers presented glass transition temperatures (T_G) of 97 and 100 °C for PS_{91}-Br and PS_{122}-Br, respectively. On the other hand, with the formation of PS-*b*-PVP copolymers, T_G values for the PS block increased about 5 °C in relation to the respective homopolymers, due to the increase in the molecular weight as well as the presence of the second rigid block. In the case of the PVP block, the T_G values obtained for both copolymers was around 167 °C. Furthermore, in Figure 3, the transition around 167 °C is more defined for the PS_{91}-*b*-PVP_{73} than for the PS_{122}-*b*-PVP_{70} copolymer. This result is in agreement with PVP ratio present in each block copolymer, since the PS_{91}-*b*-PVP_{73} copolymer presented a higher PVP content and the transition around 167 °C was consequently easier to be detected for this block copolymer. Therefore, the PS-*b*-PVP copolymers showed two distinct T_G values, which are close to the values of the corresponding PS and PVP homopolymers, indicating that PS and PVP blocks are immiscible.

3.2 Use of PS-b-PVP as a AgNP stabilizing agent

According to the previous section, the produced block copolymers presented hydrophobic to hydrophilic ratio suitable to act as a stabilizing agent (hydrophobic:hydrophilic block ratios were approximately 1:1 and 2:1). PVP is a well-known polymer used as a stabilizing agent to produce metallic (e.g. silver, gold, etc) nanoparticles[39]. In the case of amphiphilic PS-*b*-PVP copolymer, PVP block can be used as stabilizing and co-reducing agents while the PS block can act as a hydrophobic segment. In this case, the amphiphilic PS-*b*-PVP copolymer can be used as a compatibilizer agent for polymeric matrices, mainly to those containing PS or a polymer miscible with PS.

The synthesis of AgNP stabilized by PS-*b*-PVP (AgNP/PS-*b*-PVP) was carried out by the direct addition of $AgNO_3$ into the system (DMAc, NaOH and block copolymer). After $AgNO_3$ addition, the solution turned yellowish indicating the successful formation of AgNP/PS-*b*-PVP in a unique step. In the present work, the PVP block size of both PS_{91}-*b*-PVP_{73} and PS_{122}-*b*-PVP_{70} copolymers synthesized are around 8,000 g mol^{-1}, thus AgNP can be produced with any of the block copolymer synthesized in this work.

Park et al.[19] synthesized the PS-*b*-PVP block copolymer (M_w = 20,000 g mol^{-1}, PS mass fraction of 0.70 and Đ = 1.4) by ATRP using anisol as a solvent. The authors prepared a polymer solution dissolving PS-*b*-PVP (1 wt%) in THF. $AgCF_3CO_3$ (20 wt% with respect to block copolymer) was solubilized in the polymer solution and then the polymer/salt solution was dropped and spread on a glass slide in order to form a film. The glass slide containing the PS-*b*-PVP/$AgCF_3CO_3$ film was UV irradiated (254 nm) for 1 h when the authors observed the AgNP/PS-*b*-PVP formation. The nanoparticles presented 4-6 nm average diameter, although UV-vis showed a broad band with low intensity. In this above related work, the AgNP were produced from two different steps: (i) PS-*b*-PVP/$AgCF_3CO_3$ film formation and (ii) posterior UV film irradiation. The PS-*b*-PVP synthesized by Park et al.[19] is very similar to PS_{122}-*b*-PVP_{70}

synthesized in the present work (M_w = 19,000 g mol^{-1}, PS mass fraction of 0.64 and Đ = 1.4). However, in this work, a one-step methodology was used to produce AgNP stabilized by PS-*b*-PVP copolymers.

The ultraviolet-visible (UV-vis) spectrum was used to confirm the formation of AgNP/PS-*b*-PVP. Only one absorption band with a 410 nm maximum absorbance was observed in the UV-vis spectrum presented in Figure 4a, confirming the characteristic silver surface plasmon[40,41] as well as the fact that the nanoparticles were spherical. The dispersity of colloidal suspension was evaluated by the full width at half maximum (FWHM) and the obtained value was 62 nm, which indicates that the AgNP/PS-*b*-PVP can be considered monodispersed[42]. Typical AgNP/PS-*b*-PVP EF-TEM image are shown in Figure 4b, which present spherical monodisperse nanoparticles. These findings corroborate the UV-vis results. Furthermore, the AgNP/PS-*b*-PVP diameter were measured from EF-TEM images and size distribution is shown in Figue 4 (c). The nanoparticle size distribution presented an 11 ± 1 nm average diameter.

The AgNP/PS_{122}-*b*-PVP_{70} were dried by lyophilization and submitted to a simple test: the AgNP/PS_{122}-*b*-PVP_{70} was added to ethanol and sonicated for 10 minutes. After sonification, no AgNP redispersion was observed as shown in Figure 5a. However, removing ethanol and adding DMAc to the same container, the AgNP redispersion occurred immediately, as shown in Figure 5 (b). This simple test macroscopically demonstrates that the AgNP have an hydrophobic shell (PS block), which differentiates the AgNP produced in this work from the classical AgNP stabilized by PVP[11,43,44]. Thus, we can propose that there is a polymeric bilayer encapsulating the AgNP where the PVP block forms the inner layer and is responsible for the silver nanoparticle stabilization, while the PS block forms the outer layer which provides a hydrophobic character to the nanoparticle external surface. For this reason, AgNP stabilized by PS-*b*-PVP copolymers do not redisperse in ethanol.

The AgNP/PS-*b*-PVP colloidal suspensions were maintained unstirred in the dark for several weeks. No agglomeration was observed after 60 days, indicating that the PS-*b*-PVP copolymers provided stable AgNP suspensions.

3.3 Use of PS-b-PVP copolymer as surface modifier agent of SiO_2NP

Another application for the synthesized PS-*b*-PVP copolymer is a surface modifying agent. SiO_2NP prepared by the Stöber method[29] was used to demonstrate this property. Nanoparticles prepared by this method presented diameters around 72 ± 9 nm. For this test, the PS-*b*-PVP solution was directly added to the SiO_2NP/DMAc dispersions to promote copolymer adsorption on the nanoparticle surface.

The PVP adsorption onto silica surface is attributed to the strong and spontaneous interaction between the carbonyl groups present in the amide ring and the silanol groups of the silica surface[45,46]. In relation to the adsorption of the PS-*b*-PVP copolymer on the SiO_2NP surface, the formation of a polymeric bilayer encapsulating the nanoparticle can be proposed: the PVP block adsorbs preferentially at the SiO_2NP surface, forming an inner layer, and the PS block forms an outer layer, which provides the SiO_2NP with a hydrophobic surface character.

Figure 6a and b compare EF-TEM images and elemental carbon maps of SiO_2NP and SiO_2NP modified by PS_{122}-*b*-PVP_{70} (SiO_2NP/PS_{122}-*b*-PVP_{70}), respectively. The green region in carbon maps corresponds to the carbon presence in the

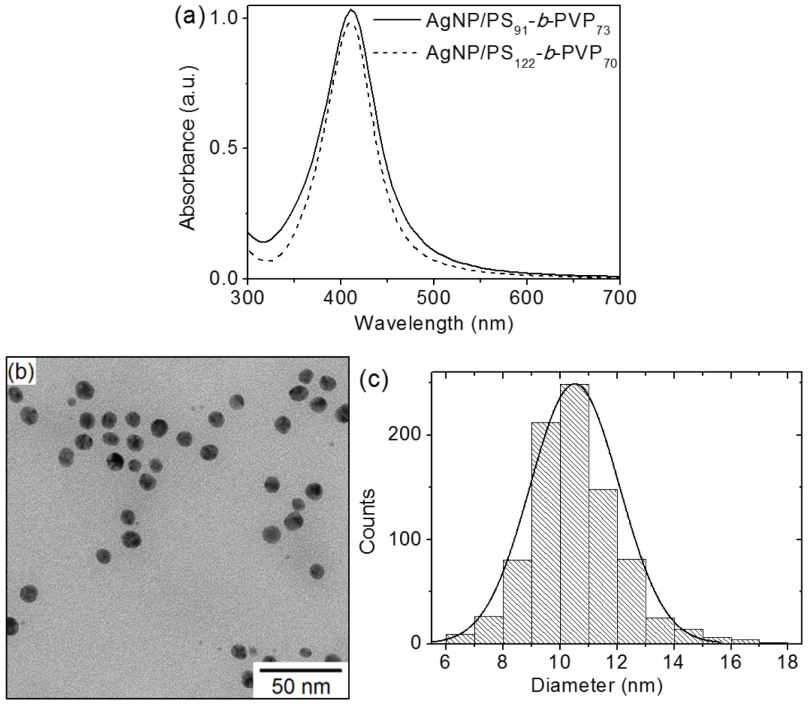

Figure 4. (a) UV-vis spectra, (b) EF-TEM image and (c) size distribution of the Ag/PS-*b*-PVP.

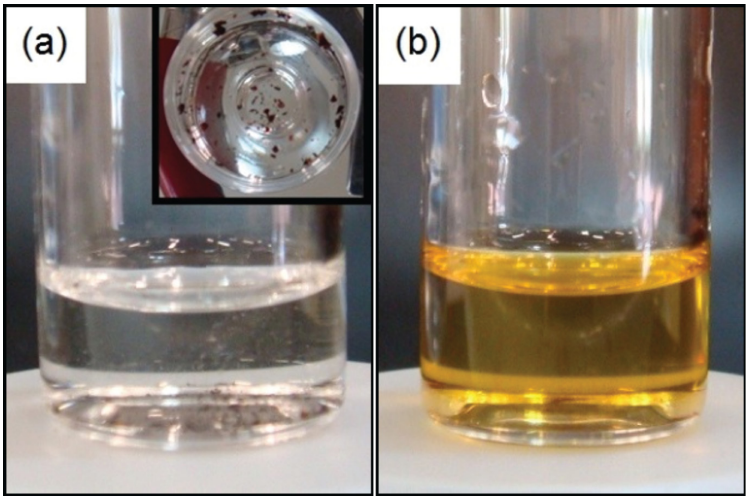

Figure 5. (a) AgNP/PS_{122}-*b*-PVP_{70} in ethanol and (b) after removing ethanol and adding DMAc. Insert in (a) shows the AgNP/PS_{122}-*b*-PVP_{70} at the flask'sbottom after sonification.

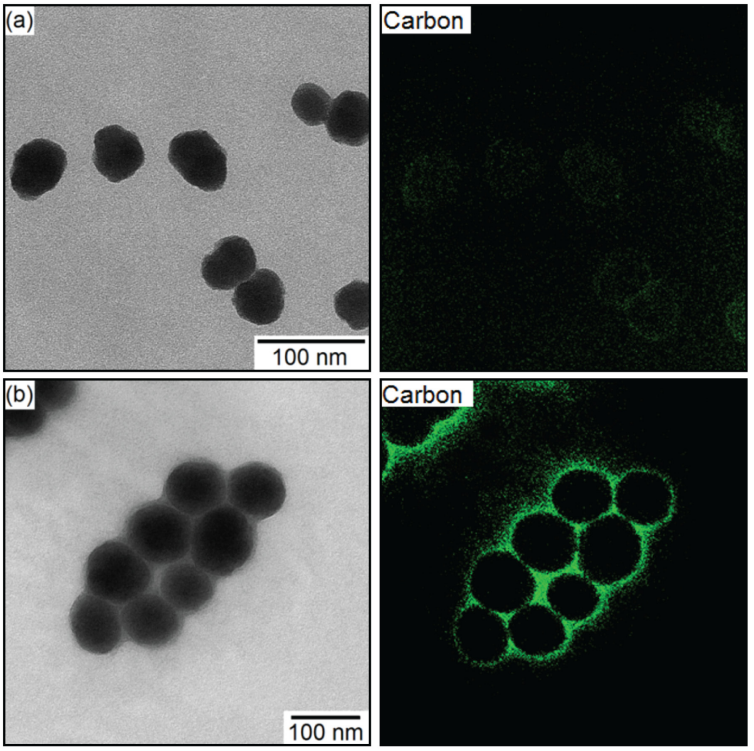

Figure 6. EF-TEM images of SiO_2NP synthesized by the Stöber method. (a) pure SiO_2NP and (b) SiO_2NP/PS_{122}-*b*-PVP_{70} with their respective carbon maps.

respective EF-TEM bright field images. The SiO_2NP carbon mapping exhibits the presence of carbon throughout the nanoparticles presented in Figure 6a. This mapping shows that the carbon content dispersed throughout the SiO_2NP was, in fact, very small and is attributed to residual non-hydrolyzed ethoxy groups from the Stöber method synthesis[30,47,48]. Van Helden et al.[49] synthesized SiO_2NP by the Stöber method and determined that the amount of non-hydrolyzed ethoxy groups was around 1 wt%.

The PS-*b*-PVP copolymer layer adsorbed onto the SiO_2NP nanoparticles can be seen in the EF-TEM image, Figure 6b. Furthermore, the corresponding carbon map of this image clearly showed the presence of a significant amount of carbon surrounding the nanoparticles (green regions), confirming the SiO_2NP surface modification by the PS-*b*-PVP copolymer. The estimated average copolymer layer thickness was 5 ± 1 nm. Freris et al.[50] obtained similar results using poly(methyl methacrylate) to encapsulate

SiO_2NP with 180 nm diameter. In the related work, the authors identified a polymeric layer with thickness between 2 and 10 nm by TEM.

4. Conclusions

PS-*b*-PVP copolymers with controlled molecular weight and relatively narrow polydispersity were synthesized using first ATRP for styrene polymerization and subsequently RAFT for N-vinyl-2-pyrrolidone polymerization. The PS-*b*-PVP copolymers presented number average molecular weight of 10,000-14,000 g mol^{-1}, $M_w/M_n \leq 1.4$ and 0.55-0.64 PS mass fraction. These PS-*b*-PVP copolymers were successfully applied as a stabilizing agent to synthesize AgNP in a single step, as confirmed by the UV-vis spectrum and EF-TEM images. No agglomeration was observed after 60 days, indicating that PS-*b*-PVP provides stable suspensions of AgNP in the organic solvent (dimethylacetamide). Furthermore, the PS-*b*-PVP copolymer also acted successfully as a surface modifying agent for the silica nanoparticles obtained by the Stöber method, as shown by EF-TEM images and elemental carbon maps. This surface modification provided SiO_2NP with a hydrophobic surface character. This work highlighted the chemical and structural importance of PS-*b*-PVP copolymers in polymer science applications. Besides the applications shown here, these copolymers could also be used as water-in-oil emulsifier or coupling agents between inorganic particles and polymeric matrices.

5. Acknowledgements

The authors thank PETROBRAS-CENPES, Brazilian agency FAPESP (FAPESP, 2010/17804-7) and National Institute of Science, Technology and Innovation in Complex Functional Materials (Inomat/INCT, FAPESP 2008/57867-8, CNPq 573644/2008-0) for the financial support. M. A. de Farias also thanks CAPES for the scholarship.

6. References

1. Wang, Z., Zhang, Q., Zhan, X., Chen, F., Rao, G., & Xiong, J. (2013). Preparation, kinetics and microstructures of well-defined PS-b-PS/Bd diblock copolymers via RAFT miniemulsion polymerization. *Journal of Polymer Research*, *20*(11), 288. http://dx.doi.org/10.1007/s10965-013-0288-0.
2. Li, G. H., Yang, P. P., Gao, Z. S., & Zhu, Y. Q. (2012). Synthesis and micellar behavior of poly(acrylic acid-b-styrene) block copolymers. *Colloid & Polymer Science*, *290*(17), 1825-1831. http://dx.doi.org/10.1007/s00396-012-2799-3.
3. Roghani-Mamaqani, H., Haddadi-Asl, V., Khezri, K., Zeinali, E., & Salami-Kalajahi, M. (2013). In situ atom transfer radical polymerization of styrene to in-plane functionalize graphene nanolayers: grafting through hydroxyl groups. *Journal of Polymer Research*, *21*(1), 333. http://dx.doi.org/10.1007/s10965-013-0333-z.
4. Wang, J.-S., & Matyjaszewski, K. (1995). Controlled/"living" radical polymerization. atom transfer radical polymerization in the presence of transition-metal complexes. *Journal of the American Chemical Society*, *117*(20), 5614-5615. http://dx.doi.org/10.1021/ja00125a035.
5. Matyjaszewski, K., Patten, T. E., & Xia, J. (1997). Controlled/"living" radical polymerization. kinetics of the homogeneous atom transfer radical polymerization of styrene. *Journal of the American Chemical Society*, *119*(4), 674-680. http://dx.doi.org/10.1021/ja963361g.
6. Aitchison, T. J., Ginic-Markovic, M., Clarke, S., & Valiyaveettil, S. (2012). Polystyrene-block-poly(methyl methacrylate): initiation issues with block copolymer formation using ARGET ATRP. *Macromolecular Chemistry and Physics*, *213*(1), 79-86. http://dx.doi.org/10.1002/macp.201100478.
7. Moad, G., Rizzardo, E., & Thang, S. H. (2005). Living radical polymerization by the RAFT process. *Australian Journal of Chemistry*, *58*(6), 379-410. http://dx.doi.org/10.1071/CH05072.
8. Lowe, A. B., & Mccormick, C. L. (2007). Reversible addition – fragmentation chain transfer (RAFT) radical polymerization and the synthesis of water-soluble (co)polymers under homogeneous conditions in organic and aqueous media. *Polymer*, *32*, 283-351. http://dx.doi.org/10.1016/j.progpolymsci.2006.11.003.
9. Liu, X., Wu, Z., Zhou, F., Li, D., & Chen, H. (2010). Poly(vinylpyrrolidone-b-styrene) block copolymers tethered surfaces for protein adsorption and cell adhesion regulation. *Colloids and Surfaces. B, Biointerfaces*, *79*(2), 452-459. http://dx.doi.org/10.1016/j.colsurfb.2010.05.011. PMid:20554165.
10. Kumar, S., Changez, M., Murthy, C. N., Yamago, S., & Lee, J.-S. (2011). Synthesis of well-defined amphiphilic block copolymers by organotellurium-mediated living radical polymerization (TERP). *Macromolecular Rapid Communications*, *32*(19), 1576-1582. http://dx.doi.org/10.1002/marc.201100277. PMid:21793088.
11. Zhang, Z., Zhao, B., & Hu, L. (1996). PVP protective mechanism of ultrafine silver powder synthesized by chemical reduction processes. *Journal of Solid State Chemistry*, *121*(1), 105-110. http://dx.doi.org/10.1006/jssc.1996.0015.
12. Riess, G. (2003). Micellization of block copolymers. *Progress in Polymer Science*, *28*(7), 1107-1170. http://dx.doi.org/10.1016/S0079-6700(03)00015-7.
13. Hamley, I. W. (1998). *The physics of block copolymers*. Oxford: Oxford University Press.
14. Xue, B., Gao, L., Hou, Y., Liu, Z., & Jiang, L. (2013). Temperature controlled water/oil wettability of a surface fabricated by a block copolymer: application as a dual water/oil on-off switch. *Advanced Materials*, *25*(2), 273-277. http://dx.doi.org/10.1002/adma.201202799. PMid:23074035.
15. Uyen, N. T. N., Joo, S. I., Kim, W. H., Oh, M. H., Lee, J., Lim, B. S., & Hong, S. C. (2013). Application of block copolymeric surface modifier with crosslinkable units for montmorillonite nanocomposites. *Journal of Applied Polymer Science*, *127*(1), 690-698. http://dx.doi.org/10.1002/app.37856.
16. Zhang, D., Qi, L., Ma, J., & Cheng, H. (2001). Formation of silver nanowires in aqueous solutions of a double-hydrophilic block copolymer. *Chemistry of Materials*, *13*(9), 2753-2755. http://dx.doi.org/10.1021/cm0105007.
17. Li, N., Qi, L., Shen, Y., Li, Y., & Chen, Y. (2013). Amphiphilic block copolymer modified magnetic nanoparticles for microwave-assisted extraction of polycyclic aromatic hydrocarbons in environmental water. *Journal of Chromatography. A*, *1316*, 1-7. http://dx.doi.org/10.1016/j.chroma.2013.09.030. PMid:24119754.
18. Shamenkova, O. A., Mokeeva, L. K., Kopylova, N. A., & Semchikov, Y. D. (2006). Synthesis of amphiphilic block copolymers polystyrene-block-polyvinylpyrrolidone from active polystyrene. *Russian Journal of Applied Chemistry*, *79*(3), 448-452. http://dx.doi.org/10.1134/S1070427206030232.
19. Park, J. T., Koh, J. H., Lee, K. J., Seo, J. A., Min, B. R., & Kim, J. H. (2008). Formation of silver nanoparticles created in situ in an amphiphilic block copolymer film. *Journal of Applied Polymer Science*, *110*(4), 2352-2357. http://dx.doi.org/10.1002/app.28261.
20. Hussain, H., Tan, B. H., Gudipati, C. S., Liu, Y., He, C. B., & Davis, T. P. (2008). Synthesis and self-assembly of poly(styrene)-

b-poly(N-vinylpyrrolidone) amphiphilic diblock copolymers made via a combined ATRP and MADIX approach. *Journal of Polymer Science. Part A, Polymer Chemistry*, *46*(16), 5604-5615. http://dx.doi.org/10.1002/pola.22882.

21. Hu, D., & Zheng, S. (2010). Reaction-induced microphase separation in polybenzoxazine thermosets containing poly(N-vinyl pyrrolidone)-block-polystyrene diblock copolymer. *Polymer*, *51*(26), 6346-6354. http://dx.doi.org/10.1016/j.polymer.2010.10.047.
22. Huang, C.-F., Nicolaÿ, R., Kwak, Y., Chang, F.-C., & Matyjaszewski, K. (2009). Homopolymerization and block copolymerization of N-vinylpyrrolidone by ATRP and RAFT with haloxanthate inifers. *Macromolecules*, *42*(21), 8198-8210. http://dx.doi.org/10.1021/ma901578z.
23. Bilalis, P., Pitsikalis, M., & Hadjichristidis, N. (2006). Controlled nitroxide-mediated and reversible addition-fragmentation chain transfer polymerization of N-vinylpyrrolidone: Synthesis of block copolymers with styrene and 2-vinylpyridine. *Journal of Polymer Science. Part A, Polymer Chemistry*, *44*(1), 659-665. http://dx.doi.org/10.1002/pola.21198.
24. Arsalani, N., Fattahi, H., & Entezami, A. A. (2006). Synthesis of amphiphilic diblock and random copolymers of styrene and N-vinylpyrrolidone using nitroxide-mediated living free radical polymerization. *Iranian Polymer Journal*, *15*(12), 997-1005. Retrieved in 16 January 2015, from http://www.sid.ir/en/vewssid/j_pdf/81320061207.pdf
25. Ray, B., Kotani, M., & Yamago, S. (2006). Highly controlled synthesis of poly(N-vinylpyrrolidone) and its block copolymers by organostibine-mediated living radical polymerization. *Macromolecules*, *39*(16), 5259-5265. http://dx.doi.org/10.1021/ma060248u.
26. Zakharova, O. G., Golyagina, Y. V., & Semchikov, Y. D. (2009). Synthesis and surface properties of amphiphilic block copolymers polyvinylpyrrolidone-block-polystyrene. *Russian Journal of Applied Chemistry*, *82*(4), 644-649. http://dx.doi.org/10.1134/S107042720904020X.
27. Wager, C. M., Haddleton, D. M., & Bon, S. A. (2004). A simple method to convert atom transfer radical polymerization (ATRP) initiators into reversible addition fragmentation chain-transfer (RAFT) mediators. *European Polymer Journal*, *40*(3), 641-645. http://dx.doi.org/10.1016/j.eurpolymj.2003.10.025.
28. Hayes, W., & Rannard, S. (2004). *Controlled/"living" polymerization methods*. In F. J. Daves (Ed.). *Polymer synthesis – a practical approach* (pp. 99-125). New York: Oxford University Press.
29. Stöber, W., Fink, A., & Bohn, E. (1968). Controlled growth of monodisperse silica spheres in the micron size range. *Journal of Colloid and Interface Science*, *26*(1), 62-69. http://dx.doi.org/10.1016/0021-9797(68)90272-5.
30. Costa, C. A. R., Leite, C. A. P., & Galembeck, F. (2003). Size dependence of Stöber silica nanoparticle microchemistry. *The Journal of Physical Chemistry B*, *107*(20), 4747-4755. http://dx.doi.org/10.1021/jp027525t.
31. Mark, J. E. (1999). *Polymer data handbook*. New York: Oxford University Press.
32. Williams, D., & Fleming, I. (2007). *Spectroscopic methods in organic chemistry* (6th ed.). New York: McGraw-Hill Higher Education.
33. Wan, D., Satoh, K., Kamigaito, M., & Okamoto, Y. (2005). Xanthate-mediated radical polymerization of N-vinylpyrrolidone in fluoroalcohols for simultaneous control of molecular weight and tacticity. *Macromolecules*, *38*(25), 10397-10405. http://dx.doi.org/10.1021/ma0515230.
34. Wang, J.-S., & Matyjaszewski, K. (1995). Controlled/"living" radical polymerization. Halogen atom transfer radical polymerization promoted by a Cu(I)/Cu(II) redox process. *Macromolecules*, *28*(23), 7901-7910. http://dx.doi.org/10.1021/ma00127a042.
35. Matyjaszewski, K., & Xia, J. (2001). Atom transfer radical polymerization. *Chemical Reviews*, *101*(9), 2921-2990. http://dx.doi.org/10.1021/cr940534g. PMid:11749397.
36. Perrier, S., & Takolpuckdee, P. (2005). Macromolecular design via reversible addition-fragmentation chain transfer (RAFT)/xanthates (MADIX) polymerization. *Journal of Polymer Science. Part A, Polymer Chemistry*, *43*(22), 5347-5393. http://dx.doi.org/10.1002/pola.20986.
37. Kahveci, M. U., Acik, G., & Yagci, Y. (2012). Synthesis of block copolymers by combination of atom transfer radical polymerization and visible light-induced free radical promoted cationic polymerization. *Macromolecular Rapid Communications*, *33*(4), 309-313. http://dx.doi.org/10.1002/marc.201100641. PMid:22253209.
38. Chavda, S., Yusa, S., Inoue, M., Abezgauz, L., Kesselman, E., Danino, D., & Bahadur, P. (2013). Synthesis of stimuli responsive PEG47–b-PAA126–b-PSt32 triblock copolymer and its self-assembly in aqueous solutions. *European Polymer Journal*, *49*(1), 209-216. http://dx.doi.org/10.1016/j.eurpolymj.2012.09.021.
39. Wang, H., Qiao, X., Chen, J., Wang, X., & Ding, S. (2005). Mechanisms of PVP in the preparation of silver nanoparticles. *Materials Chemistry and Physics*, *94*(2-3), 449-453. http://dx.doi.org/10.1016/j.matchemphys.2005.05.005.
40. Noguez, C. (2007). Surface plasmons on metal nanoparticles: the influence of shape and physical environment. *The Journal of Physical Chemistry C*, *111*(10), 3806-3819. http://dx.doi.org/10.1021/jp066539m.
41. Indumathy, R., Sreeram, K. J., Sriranjani, M., Aby, C. P., & Nair, B. U. (2010). Bifunctional role of thiosalicylic acid in the synthesis of silver nanoparticles. *Materials Sciences and Applications*, *1*(05), 272-278. http://dx.doi.org/10.4236/msa.2010.15040.
42. Medina-Ramirez, I., Bashir, S., Luo, Z., & Liu, J. L. (2009). Green synthesis and characterization of polymer-stabilized silver nanoparticles. *Colloids and Surfaces. B, Biointerfaces*, *73*(2), 185-191. http://dx.doi.org/10.1016/j.colsurfb.2009.05.015. PMid:19539451.
43. Lee, J.-M., Jun, Y.-D., Kim, D.-W., Lee, Y.-H., & Oh, S.-G. (2009). Effects of PVP on the formation of silver–polystyrene heterogeneous nanocomposite particles in novel preparation route involving polyol process: Molecular weight and concentration of PVP. *Materials Chemistry and Physics*, *114*(2-3), 549-555. http://dx.doi.org/10.1016/j.matchemphys.2008.10.001.
44. Wiley, B. J., Im, S. H., Li, Z.-Y., McLellan, J., Siekkinen, A., & Xia, Y. (2006). Maneuvering the surface plasmon resonance of silver nanostructures through shape-controlled synthesis. *The Journal of Physical Chemistry B*, *110*(32), 15666-15675. http://dx.doi.org/10.1021/jp0608628. PMid:16898709.
45. Cohen Stuart, M., Fleer, G., & Bijsterbosch, B. (1982). The adsorption of poly(vinyl pyrrolidone) onto silica. I. Adsorbed amount. *Journal of Colloid and Interface Science*, *90*(2), 310-320. http://dx.doi.org/10.1016/0021-9797(82)90300-9.
46. Robinson, S., & Williams, P. A. (2002). Inhibition of protein adsorption onto silica by polyvinylpyrrolidone. *Langmuir*, *18*(23), 8743-8748. http://dx.doi.org/10.1021/la020376l.
47. Costa, C. A. R., Leite, C. A. P., & Galembeck, F. (2006). ESI-TEM imaging of surfactants and ions sorbed in Stöber silica nanoparticles. *Langmuir*, *22*(17), 7159-7166. http://dx.doi.org/10.1021/la060389p. PMid:16893211.
48. Costa, C. A. R., Valadares, L. F., & Galembeck, F. (2007). Stöber silica particle size effect on the hardness and brittleness of silica monoliths. *Colloids and Surfaces. A, Physicochemical and Engineering Aspects*, *302*(1-3), 371-376. http://dx.doi.org/10.1016/j.colsurfa.2007.02.061.

49. Van Helden, A. K., Jansen, J. W., & Vrij, A. (1981). Preparation and characterization of spherical monodisperse silica dispersions in nonaqueous solvents. *Journal of Colloid and Interface Science*, *81*(2), 354-368. http://dx.doi.org/10.1016/0021-9797(81)90417-3.
50. Freris, I., Cristofori, D., Riello, P., & Benedetti, A. (2009). Encapsulation of submicrometer-sized silica particles by a thin shell of poly(methyl methacrylate). *Journal of Colloid and Interface Science*, *331*(2), 351-355. http://dx.doi.org/10.1016/j.jcis.2008.11.052. PMid:19081575.

Received: Jan. 16, 2015
Revised: Aug. 13, 2015
Accepted: Aug. 17, 2015